Bacterial oxidation of ferrous iron by *Acidithiobacillus ferrooxidans* in the pH range 2.5–7.0

Gabriel Meruane, Tomás Vargas*

Centro de Hidrometalúrgia/Electrometalúrgia (CHEM-CHILE), Depto. de Ingeniería de Minas, Universidad de Chile, Tupper 2069 Santiago, Chile
Depto. de Ingeniería Química, Universidad de Chile, Tupper 2069 Santiago, Chile

Abstract

The oxidation of ferrous iron by *Acidithiobacillus ferrooxidans* in the pH range 2.5–7.0 was characterized. In order to measure the rate of bacterial oxidation of ferrous iron with *A. ferrooxidans* in this high pH range, a novel experimental methodology was developed. The results showed that the inhibition of ferrous iron oxidation activity by *A. ferrooxidans* observed at pH values above 3.0 is partially linked to the formation of ferric iron precipitates, which apparently hinder transport processes on the cell surface. By carefully controlling the amount of iron precipitates formed during the oxidation of ferrous iron in this pH range, enhanced bacterial activity was obtained.

Keywords: *Acidithiobacillus ferrooxidans*; Ferrous iron oxidation; Bioleaching; Bacterial activity; Iron precipitation

1. Introduction

The main mechanism of bacterial catalysis in the dissolution of sulfide minerals is based on the bacterial oxidation of ferrous iron, with oxygen as electron acceptor, according to the reaction:

$$Fe^{2+} + 1/4\ O_2 + H^+ \rightarrow Fe^{3+} + 1/2\ H_2O \qquad (1)$$

It is known that ferrous iron oxidation by *Acidithiobacillus ferrooxidans* rapidly decreases at pH greater than 2.5 (Nakamura et al., 1986; Pesic et al., 1989; Kupka and Kupsáková, 1999). In most reports of ferrous iron oxidation by acidophiles, bacterial catalysis is significant only up to pH ~ 3.5 (MacDonald and Clark, 1970; Pesic et al., 1989; Kupka and Kupsáková, 1999). According to the chemiosmotic theory, a decrease in the ferrous iron oxidation activity of *A. ferrooxidans* is expected when the pH increases (Ingledew, 1982). Some authors have suggested that the formation of ferric iron precipitates can also have an inhibiting influence in this pH range (Nemati et al., 1998; Espejo et al., 1988), though there is no clear evidence to support this suggestion. This lack of understanding is related to the limitations of the current methodologies, which prevent accurate measurements of bacterial ferrous iron oxidation rate at pH over 3.0. Current measurements are mainly based on the monitoring of ferrous iron concentration decrease, oxygen consumption or Eh evolution (MacDonald and Clark,

* Corresponding author. Centro de Hidrometalúrgia/Electrometalúrgia (CHEM/CHILE), Depto. de Ingeniería de Minase Ingeniería Química, Universidad de Chile, Tupper 2069 Santiago, Chile. Tel.: +56-2-6784283; fax: +56-2-6991084.
E-mail address: tvargas@cec.uchile.cl (T. Vargas).

1970; Pesic et al., 1989; Kupka and Kupsáková, 1999). These methods are not directly applicable at high pH ranges, where ferrous iron oxidation is accompanied by rapid variations of pH and total iron concentration.

In the present work, the bacterial oxidation of ferrous iron in the pH range 2.5–7.0 was investigated. A novel experimental methodology was developed to evaluate bacterial activity over this pH range. This approach permitted the separate evaluation of the inhibiting effects of both proton concentration depletion and ferric iron precipitation (linked to pH increase) on bacterial ferrous iron oxidation.

2. Materials and methods

2.1. Bacterial culture preparation

A pure strain of *A. ferrooxidans* (ATCC 19859) was used in the study. The bacteria were cultured in 250-mL Erlenmeyer flasks containing 100 mL of medium with the composition: 0.4 g/L $(NH_4)_2SO_4$, 0.4 g/L $MgSO_4 \cdot 7H_2O$, 0.056 g/L $K_2HPO_4 \cdot 3H_2O$, 14.9 g/L $FeSO_4 \cdot 7H_2O$ (Touvinen and Kelly, 1973). The pH of the medium was adjusted to 1.6 using sulfuric acid, and cultures were incubated, shaken, at 30 °C. The bacteria were maintained in the exponential growth phase by daily subculturing 20% of the solution.

The inoculum to be used in each experimental run was prepared from 80 mL of culture sample, which was filtered through a 0.22-μm Millipore® membrane. The bacterial pellet was washed four times: twice with 20 mL of pH 1.6 sulfuric acid solution for iron removal and twice with distilled water to remove residual acid. It was then resuspended in 10 mL of pH 6.0 distilled water or iron-free basal medium. The cell population in this inoculum, determined by direct counting using a Petroff–Hausser chamber, was typically in the range of $8–10 \times 10^8$ cells/mL.

2.2. Experimental assembly and procedure

The abundant precipitate formation and rapid variations in pH that are associated with the oxidation of ferrous iron at pH>2.3 preclude accurate measurements of the bacterial oxidation process by direct measurement of variations of ferrous iron concentrations in solution. Consequently, a novel method was developed to determine the rate of ferrous iron oxidation from the data of the evolution of Eh and pH during the oxidation process.

The scheme of the experimental set-up is shown in Fig. 1. The cell contained 25 mL of the test solution in which a combined pH electrode (Sensorex S201C) and a combined Eh electrode (Cole-Palmer 5990-57), which uses Ag/AgCl (sat) as reference electrode, were immersed. Both electrodes were connected to a data acquisition system Opto 22 that measured the potential difference in both electrodes and sent the data to an IBM-compatible PC that registers the pH and Eh variations with time. In order to avoid the short circuit of signals, only one of the reference electrodes was electrically connected, and the values of both the pH and Eh electrodes were referred to it. The solution in the cell was agitated using a magnetic stirrer, and the cell was maintained at a constant temperature of 30 ± 1 °C using a water-heating jacket.

The test solution was prepared in situ according to the following procedure: 25 mL of iron-free basal medium was initially added to the cell and deoxygenated by the continuous bubbling of high-purity nitro-

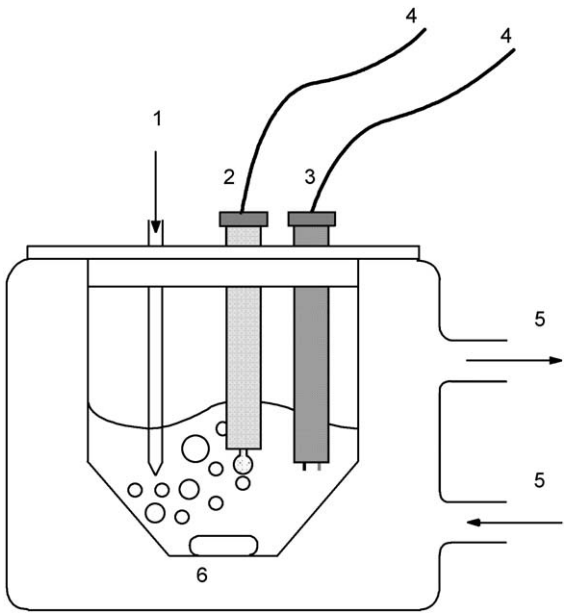

Fig. 1. Experimental assembly. (1) Air/N_2 bubbling; (2) pH electrode; (3) Eh electrode; (4) data acquisition system; (5) thermostatized water circuit; (6) magnetic stirrer.

gen. Next, 1 M NaOH solution was added dropwise until a pH slightly over 7.0 was obtained. Whilst still under nitrogen bubbling, a predetermined amount of ferrous sulfate was added to reach the initial desired ferrous iron concentration (1 g/L). This procedure enabled the solubilization of ferrous iron to occur at high pH completely preventing its spontaneous oxidation. If required, some additional NaOH was added to readjust the solution to pH = 7.0. Finally, bacteria, resuspended in about 1 mL of distilled water, were added to give an initial bacterial concentration of 2×10^7 cells/mL. Ferrous iron oxidation was initiated by switching from nitrogen bubbling to air bubbling. All the experiments were conducted with 1 g/L initial ferrous iron concentration, and at four different initial bacterial concentrations: 8×10^6, 2×10^7, 5×10^7, and 8×10^7 cells/mL. A blank experiment in abiotic conditions with the same initial ferrous iron concentration was also conducted. Every experimental run was conducted in duplicate. Ferrous iron oxidation rates were determined from the data of the evolution of Eh and pH, according to a calculation procedure described below.

3. Results and discussion

3.1. Calculation methodology

In every experiment, a continuous pH decrease and Eh increase was observed, which was triggered by the oxidation of ferrous iron, either by a chemical or microbiologically mediated mechanism. A typical trend is shown in Fig. 2, which corresponds to the case of an inoculated basal medium solution containing an initial ferrous iron concentration of 1 g/L. Shifting of the Eh towards more positive values is directly related to the net increase of the Fe^{3+}/Fe^{2+} ratio in solution. Shifting of the pH towards acidic values results from the balance between the simultaneous consumption of protons in the oxidation of ferrous iron and the release of protons related to ferric iron precipitation. A calculation procedure to determine the rate of ferrous iron oxidation from the variations of Eh and pH was developed, as described below.

The oxidation of ferrous iron can be expressed by the reaction described in Eq. (1). Using the methodology proposed by Byrne and Luo (2000), it was experimentally shown that the ferric iron precipitation process in the basal medium could be described by the following stoichiometry (Meruane, 2002):

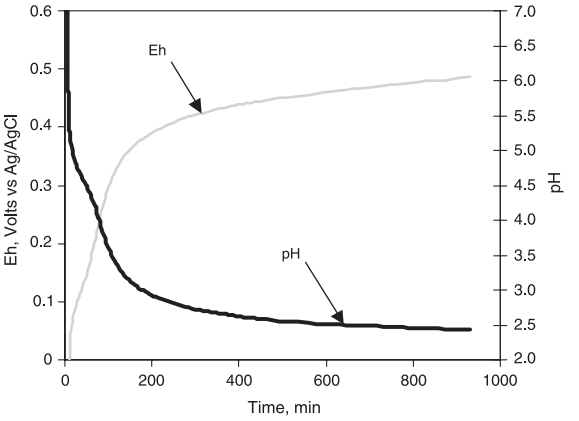

Fig. 2. Evolution of Eh and pH. Initial bacterial population: 2×10^7 cells/mL. Initial ferrous iron concentration: 1 g/L.

$$X^+ + 3\ Fe^{3+} + 2\ SO_4^{2-} + 6\ H_2O \rightarrow XFe_3(SO_4)_2(OH)_6 + 6\ H^+ \quad (2)$$

where X^+ corresponds to a monovalent cation. This stoichiometry provides the numerical relation between moles of precipitated iron and moles of released protons to be used in the calculations.

If the rate of ferrous iron oxidation is defined as:

$$\frac{d[Fe^{2+}]}{dt} = -V_{Fe^{2+}} \quad (3)$$

and the rate of ferric iron precipitation is defined as:

$$\frac{d[Fe^{tot}]}{dt} = -V_{ppt} \quad (4)$$

then, the mass balances for Fe^{3+} and H^+ in solution are given by the equations:

$$Fe^{3+}: \quad \frac{d[Fe^{3+}]}{dt} = V_{Fe^{2+}} - V_{ppt} \quad (5)$$

$$H^+: \quad \frac{d[H^+]}{dt} = -V_{Fe^{2+}} + 2V_{ppt} \quad (6)$$

Therefore, $V_{Fe^{2+}}$ and V_{ppt} can be expressed as:

$$V_{Fe^{2+}} = \frac{d[H^+]}{dt} + 2\frac{d[Fe^{3+}]}{dt} \quad (7)$$

$$V_{ppt} = \frac{d[H^+]}{dt} + \frac{d[Fe^{3+}]}{dt} \quad (8)$$

A preliminary calibration procedure was developed to obtain explicit data of $[H^+]$ and $[Fe^{3+}]$ from the values of Eh and pH. For this purpose, the Nernst equation, which relates the solution redox potential with the ferric/ferrous ratio in solution, as obtained, giving at 30 °C:

$$Eh = 0.471 + 0.0579 \log\left(\frac{[Fe^{3+}]}{Fe^{2+}}\right) \quad (9)$$

This equation proved to be valid in the pH range 1.4–2.0 and total iron concentration range 0.1–1 g/L.

From calibration of the pH electrode, the following expression, which relates the potential signal (ΔV) to H^+ concentration, was obtained:

$$\Delta V = 0.4092 + 0.056 \log([H^+]) \quad (10)$$

The concentrations of ferric iron and ferrous iron were calculated from values of $[Fe^{tot}]$ and Eh at each time during the experiment using the following expressions:

$$R = \frac{[Fe^{3+}]}{[Fe^{2+}]} = 10^{\left(\frac{Eh-0.471}{0.579}\right)} \quad (11)$$

$$[Fe^{3+}] = \frac{R}{1+R}[Fe^{tot}] \quad (12)$$

$$[Fe^{2+}] = \frac{[Fe^{tot}]}{1+R} \quad (13)$$

Ferrous iron oxidation rate and ferric iron precipitation rate were evaluated, according to Eqs. (7) and (8), by calculating at each time the instantaneous variation of ferric iron and protons concentrations.

The total ferric iron precipitated at each time was calculated using the following equation:

$$[Fe^{ppt}] = V_T \int_0^t V_{ppt} dt \quad (14)$$

Finally, the total iron concentration to be used in the next time step was evaluated using the expression:

$$[Fe^{tot}]_t = [Fe^{tot}]_0 - [Fe^{ppt}]/V_T \quad (15)$$

The validity of the proposed calculation methodology was assessed by comparing at the end of each experiment the final iron concentration calculated according to Eq. (15) from the evolution of Eh and pH (see Fig. 2) with that determined by atomic absorption in the final solution. Calculated iron concentrations presented a deviation that was always less than 10% with respect to the experimental values. This result demonstrated the reliability of the procedure proposed for determining ferrous iron oxidation rates.

3.2. Ferrous iron oxidation rates

Results of the calculated rates of ferrous iron oxidation for the experiment with 1 g/L initial ferrous iron concentration are shown in Fig. 3 (abiotic oxidation) and Fig. 4 (biologically enhanced oxidation). The data represented correspond to values of instantaneous oxidation rates as a function of the pH, which continuously decreased with time from the initial value of 7.0.

Results in Fig. 3 for abiotic conditions show that, in this high pH range, there is a significant rate of chemical ferrous iron oxidation. In the pH range 5.5–7.0, this rate is practically constant, but at pH below 5.5, the oxidation rate rapidly declines as a result of the acidification of the solution.

Results in Fig. 4 for the inoculated case show that, in the pH range 5.0–7.0, the dependence of ferrous iron oxidation rate on pH in the presence of bacteria was similar to the one observed in the abiotic case. This implies that, in this pH range, ferrous iron oxidation is mainly the result of the chemical oxidation of ferrous iron. At pH below 5.0, however, in the inoculated experiment, the rate of ferrous iron oxidation increased with pH decrease, which indicates that in this range, the process is mainly related to bacterial catalysis. From comparison of the data in Fig. 4 and those in Fig. 3, it can be seen that, e.g., at pH 3.0, the rate of bacterial oxidation of ferrous iron is about 10^4 times larger than the corresponding rate of chemical oxidation.

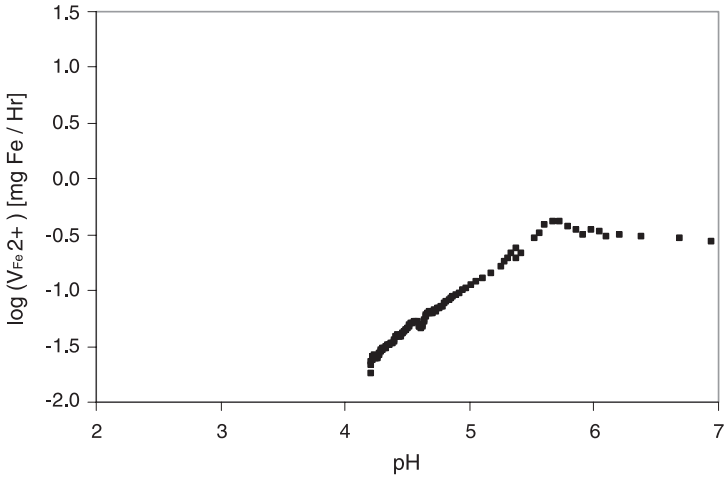

Fig. 3. Ferrous iron oxidation rate in abiotic system. $[Fe^{2+}]_{initial} = 1$ g/L.

The above results show that it is possible to determine the net rate of bacterial oxidation of ferrous iron after discounting, at each pH, the component attributable to abiotic ferrous iron oxidation. Results of bacterial oxidation of ferrous iron obtained with this procedure are shown in Fig. 5 for experiments with an initial ferrous iron concentration of 1 g/L and a varying concentration of initial inoculated bacteria. Data in Fig. 5 were then used to obtain values of V_{max}, which enabled comparison of bacterial activity determined at the four different experimental runs. For this purpose, the rate of ferrous iron oxidation was assumed to follow a Monod dependence on ferrous iron, but also included a term related to ferric iron inhibition. Then the specific ferrous iron oxidation rate ($\bar{V}_{Fe^{2+}} = V_{Fe^{2+}}/N_{bact}$) was expressed as (Liu et al., 1988):

$$\bar{V}_{Fe^{2+}} = \frac{V_{max}[Fe^{2+}]}{[Fe^{2+}] + K_S(1 + K_I[Fe^{3+}])} \tag{16}$$

where $V_{max} = \mu_{max}/Y$, Y being the yield for ferrous iron oxidation. Using this expression, values of V_{max} were

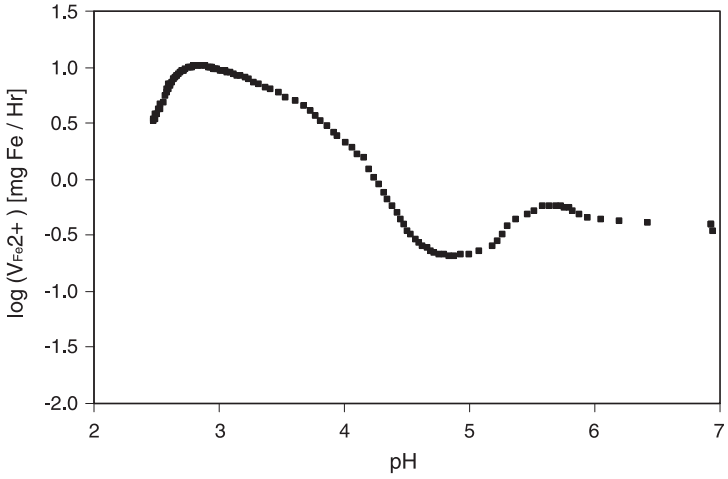

Fig. 4. Ferrous iron oxidation rate in inoculated system. $[Fe^{2+}]_{initial} = 1$ g/L. Initial bacterial population: 2×10^7 cells/mL.

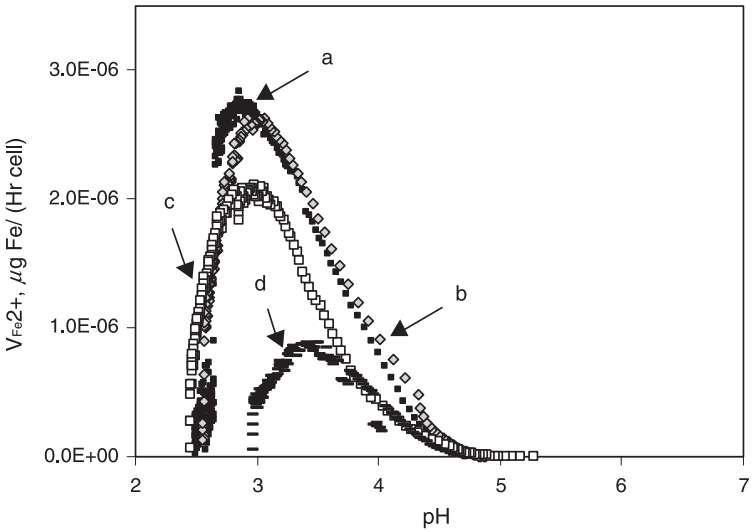

Fig. 5. Net rate of bacterial ferrous iron oxidation for experiments with different initial bacterial population. Curve a: 8×10^7 cell/mL; Curve b: 5×10^7 cell/mL; Curve c: 2×10^7 cell/mL; Curve d: 8×10^6 cell/mL. $[Fe^{2+}]_{initial} = 1$ g/L.

obtained from the values of $V_{Fe^{2+}}$ at each pH. In this calculation, the following values were used for parameters in Eq. (16) (Harvey and Crundwell, 1997): $K_S = 73$ mg/L and $K_I = 1.29 \times 10^{-3}$ L/mg. Values of V_{max} obtained with this procedure are shown in Fig. 6, which compares the behavior of experiments with different initial bacterial populations (between 8×10^6 and 8×10^7 cell/mL) and 1 g/L initial ferrous iron concentration.

3.3. Mechanism of bacterial activity inhibition

Data in Fig. 6 show first that for each experimental run, V_{max} starts to increase with pH decrease at pH

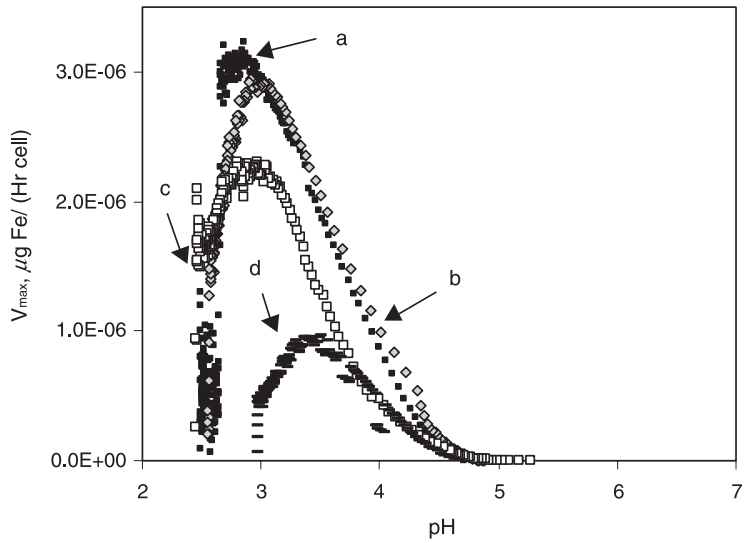

Fig. 6. Values of V_{max} for experiments with different initial bacterial population. Curve a: 8×10^7 cell/mL; Curve b: 5×10^7 cell/mL; Curve c: 2×10^7 cell/mL; Curve d: 8×10^6 cell/mL. $[Fe^{2+}]_{initial} = 1$ g/L.

below 5.0. This behavior is in agreement with the tendency predicted by the chemiosmotic theory (Ingledew, 1982). In each run, however, below a certain pH V_{max} starts to decrease with pH decrease. This last trend cannot be related to the inhibition of bacterial activity by acidity, a phenomenon that is only relevant at much lower pH (< pH 2.0) (Pesic et al., 1989; Nemati et al., 1998; Meruane, 2002). On the other hand, it is interesting to note that the measured dependence of V_{max} on pH was strongly influenced by the population of bacteria initially added to the experiment.

The possible involvement of the formation of ferric iron precipitates on the peculiar pH dependence of bacterial activity, indicated by the curvature of the line graphs in Fig. 6, was further investigated. The amounts of ferric iron precipitates that accumulated during the evolution of pH in each experiment were calculated from the expression:

$$[Fe_{sp}^{ppt}] = [Fe^{ppt}]/N_{cell} \quad (17)$$

In this expression, $[Fe_{sp}^{ppt}]$ corresponds to the specific amount of ferric iron precipitated per bacterium. $[Fe^{ppt}]$ was calculated according to Eq. (14). N_{cell}, the population of bacteria present in the flask at each time during the experiment was calculated from integration of bacteria grown out of the ferrous iron oxidation, according to the following expression:

$$N_{cell} = N_{cell}^{0} + Y \int_{t_0}^{t} V_{Fe^{2+}} dt \quad (18)$$

where t_0 is the time at which pH reaches a value about 5.0 and the bacterial oxidation starts and N_{cell}^{0} is the initial bacterial population.

Results of the calculation of $[Fe_{sp}^{ppt}]$, shown in Fig. 7, demonstrate that the amount of ferric iron precipitated per bacterium during each experiment is, in fact, larger in experiments that show relatively lower bacterial activity. These results clearly suggest that ferric iron precipitates may be playing an inhibiting role on bacterial iron oxidation. To further clarify the inhibiting influence of iron precipitates, a simple kinetic mechanism to explain its role was proposed and tested. Assuming that an important fraction of the formed ferric iron precipitates remains on the cell surface forming a compact layer, V_{max} can be expressed in terms of a mixed control kinetic mechanism involving a chemical resistance and a diffusional resistance (Levenspiel, 1962). The kinetics of the chemical reaction

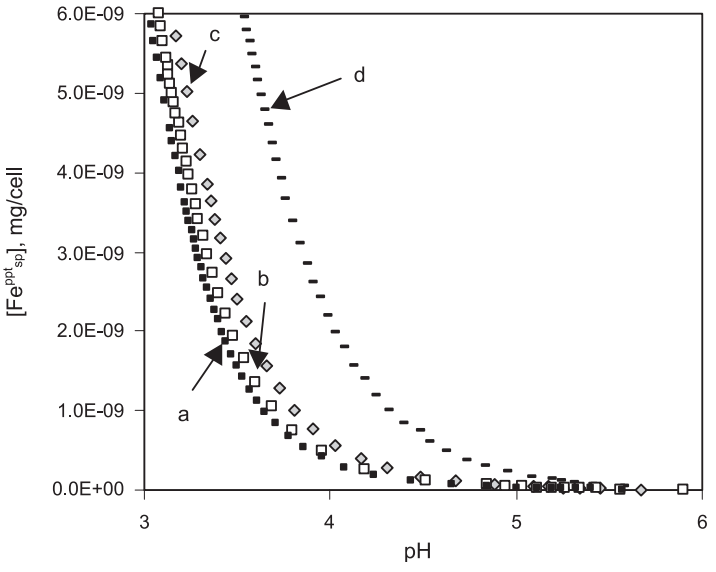

Fig. 7. Specific amount of ferric iron precipitates formed per bacteria for experiments with different initial bacterial population. Curve a: 8×10^7 cell/mL; Curve b: 5×10^7 cell/mL; Curve c: 2×10^7 cell/mL; Curve d: 8×10^6 cell/mL. $[Fe^{2+}]_{initial} = 1$ g/L.

can be related to the chemiosmotic mechanism and expressed as V^{chem}; the diffusional process can be related to diffusion of protons across the ferric iron precipitate layer formed on the bacteria. Therefore, V_{max} can be expressed as:

$$V_{max} = \frac{V^{chem}}{1 + k\Delta x} \quad (19)$$

where Δx represents the thickness of the precipitate layer and k is a constant proportional to the ratio between the diffusional and the kinetic constants. The validity of the proposed model was tested by modeling curves of V_{max} vs. pH for Runs b, c and d in Fig. 6, as a function of the amount of ferric iron precipitated. Values of V_{max} from Curve a in Fig. 6, the run with slowest $[Fe_{sp}^{ppt}]$ and larger bacterial population, were used as a pseudo-V^{chem} (here denoted as V_{ps}^{chem}). Consistent with expression (19), curves of V_{max}^{calc} vs. pH were calculated using the following formula:

$$V_{max}^{calc} = \frac{V_{ps}^{chem}}{1 + k' [Fe_{sp}^{ppt}]} \quad (20)$$

Values of k' were adjusted so that the maximum in the calculated curves equaled the maximum in the experimental curves in Fig. 6, for each experimental run.

Values of V_{max}^{calc} calculated with this procedure are shown in Fig. 8: Curves b, c and d correspond to modeling of experimental Curves b, c and d in Fig. 6; Curve a simply reproduces Curve a from Fig. 6, and is included in this figure as a reference. Results in Fig. 8 show that the calculated curves reproduce very well the tendency of V_{max}–pH curves in Fig. 6. In addition, maximum V_{max} values in each curve are located in pH values very close to the respective experimental ones. The values of k', however, are different for each calculated curve, being 2×10^7 for Curve b, 1.2×10^8 for Curve c and 1.2×10^9 for Curve d. This may be related to variations in the fraction of ferric iron precipitates that is effectively attached to the bacteria surface and/or to variations in the permeability of the passivating layer formed.

Results of the above mechanistic analysis show that the decrease in bacterial activity normally observed at pH values above 2.5 is, in fact, partially related to the formation of a layer of ferric iron precipitates on the bacteria, which hinders proton diffusion. Previous measurements of bacterial oxidation activity in this pH range with conventional methodologies have mostly been conducted using much greater ferrous iron concentrations (1–9 g/L; Nemati et al., 1998). In such cases, the inhibition observed at high pH may be related to the formation of massive amounts of ferric iron precipitates. On the

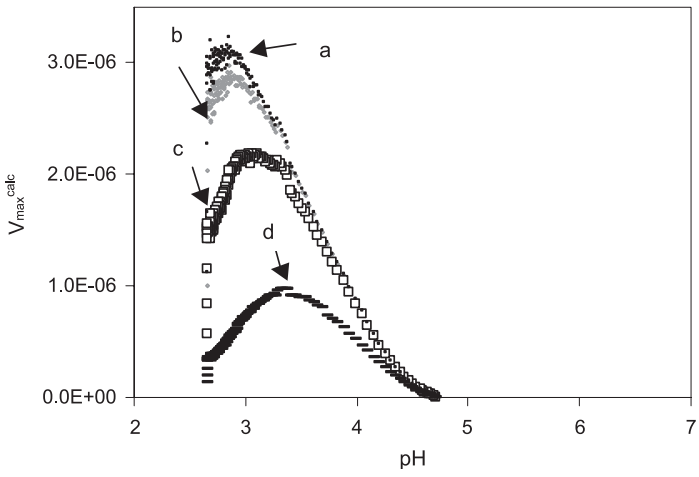

Fig. 8. Values of V_{max}^{calc} as function of pH. Curve a: 8×10^7 cell/mL (reproduction of V_{max} in Fig. 6); Curve b: 5×10^7 cell/mL; Curve c: 2×10^7 cell/mL; Curve d: 8×10^6 cell/mL.

other hand, reducing the concentration of ferrous iron can lead to a dramatic reduction of the amount of precipitates formed. As a consequence, and according to Eq. (19), this can lead to a dramatic increase of the bacterial oxidizing activity of *A. ferrooxidans* at pH above 2.5. This behavior could be probed with the use of the methodology presented in this work, which enables the determination of bacterial activity at very low ferrous iron concentrations.

Maximum rates of bacterial iron oxidation can be obtained when the formation of ferric iron precipitates is completely avoided. In this hypothetical situation, the rate of bacterial oxidation of ferrous iron will be solely controlled by the chemiosmotic mechanism. The present methodology has laid a conceptual base, which will facilitate the evaluation of the intrinsic chemiosmotic kinetics of *A. ferrooxidans*.

4. Conclusions

A novel methodology to determine the rate of ferrous iron oxidation with *A. ferrooxidans* at pH over 2.5 was developed.

At pH over 5.0, chemical oxidation predominates over bacterial oxidation of ferrous iron, and it is not possible to evaluate bacterial oxidation activity.

Bacterial oxidation of ferrous iron becomes relevant, and predominates over chemical oxidation, at pH below 5.0.

The inhibition of bacterial oxidation activity observed at pH over 2.5 is partially linked to the formation of a layer of ferric oxide precipitates on bacteria, which hinders the diffusion of protons.

It is possible to obtain noticeable improvements in the specific bacterial oxidation activity in the pH range 2.5–5.0 if a very low ferrous iron concentration is used in the experiment.

List of symbols

$[Fe^{2+}]$	Ferrous iron concentration (mg/L)
$[Fe^{3+}]$	Ferric iron concentration (mg/L)
$[Fe^{ppt}]$	Ferric iron precipitates formed (mg)
$[Fe^{ppt}_{sp}]$	Specific amount of ferric iron precipitated per bacteria (mg/cell)
$[Fe^{tot}]$	Total iron concentration (mg/L)
$[H^+]$	Proton concentration (mg/L)
k	adjustment parameter in Eq. (19) (1/m)
k'	adjustment parameter in Eq. (20) (cell/mg)
K_S	Michaelis–Menten constant (mg/L)
K_I	Ferric iron inhibition constant (no units)
N_{cell}	Bacterial concentration in solution (cell/mL)
R	Ferric to ferrous concentration ratio (no units)
V^{chem}	Maximum specific ferrous iron oxidation rate non affected by ferric precipitates (mg/h cell)
V^{chem}_{ps}	pseudo-values of V^{chem}(mg/h cell)
$V_{Fe^{2+}}$	Ferrous iron oxidation rate (mg/h)
$\bar{V}_{Fe^{2+}}$	Specific ferrous iron oxidation rate (mg/h cell)
V_{max}	Maximum specific ferrous iron oxidation rate (mg/h cell)
V^{calc}_{max}	Maximum specific ferrous iron oxidation rate calculated using V^{chem}_{ps} and $[Fe^{ppt}_{sp}]$ (mg/h cell)
V_{ppt}	Ferric iron precipitation rate (mg/h)
V_T	Total volume (0.025 L)
Y	Bacterial growth yield on ferrous iron oxidation (cell/mg Fe)
ΔV	Potential difference at the pH electrode (V vs. Ag/AgCl)
Δx	Ferric iron precipitates thickness at bacterial surface (m)

Acknowledgements

This work was conducted with the support of Fundación Andes/Fundación Antorcha grant C-13398/6. We thank CONICYT for financial support to one of us (G.M.). We are also grateful to Héctor Jordan for the helpful discussion.

References

Byrne, R.H., Luo, Y.-R., 2000. Direct observation of nonintegral hydrous ferric oxide solubility products $K^*_{SO}=[Fe^{3+}][H^+]^{-2.86}$. Geochimica et Cosmochimica Acta 64 (11), 1873–1877.

Espejo, R., Escobar, B., Jedlicki, E., Uribe, P., Badilla-Ohlbaum, R., 1988. Oxidation of ferrous iron and elemental sulfur by *Thiobacillus ferrooxidans*. Applied and Environmental Microbiology 54, 1694.

Harvey, P.I., Crundwell, F.K., 1997. Growth of *Thiobacillus ferrooxidans*: a novel experimental design for batch growth and bacterial leaching studies. Applied and Environmental Microbiology 63 (7), 2586–2592.

Ingledew, W.J., 1982. *Thiobacillus ferrooxidans*: the bioenergetics of an acidophilic chemolithotroph. Biochimica et Biophysica Acta 683, 89–117.

Kupka, D., Kupsáková, I., 1999. Iron(II) oxidation kinetics in *Thiobacillus ferrooxidans* in the presence of heavy metals. In: Amils, R., Ballester, A. (Eds.), Biohydrometallurgy and the environment toward the mining of the 21st century, Part A, Elsevier Press, Amsterdam, pp. 387–396.

Levenspiel, O., 1962. Chemical Reaction Engineering. John Wiley & Sons, New York, pp. 393–409.

Liu, M.S., Branion, R.M.R., Duncan, D.W., 1988. The effects of the ferrous iron, dissolved oxygen, and inert solids concentration on the growth of *Thiobacillus ferrooxidans*. The Canadian Journal of Chemical Engineering 66, 445–451.

MacDonald, D.G., Clark, R.H., 1970. The oxidation of aqueous ferrous sulphate by *Thiobacillus ferrooxidans*. The Canadian Journal of Chemical Engineering 48, 669–676.

Meruane, G., 2002. Oxidación bacteriana de sulfato ferroso con *Acidithiobacillus ferrooxidans*. PhD Thesis, Universidad de Chile.

Nakamura, K., Noike, T., Matsumoto, J., 1986. Effect of operation conditions on biological Fe^{2+} oxidation with rotating biological contactors. Water Resources 20 (1), 73–77.

Nemati, M., Harrison, S.T.L., Hansford, G.S., Webb, C., 1998. Biological oxidation of ferrous sulphate by *Thiobacillus ferrooxidans*: a review on kinetic aspects. Biochemical Engineering Journal 1, 171–190.

Pesic, B., Oliver, D.J., Wichlacz, P., 1989. An electrochemical method to measuring the rate of ferrous to ferric iron with oxygen in the presence of *Thiobacillus ferrooxidans*. Biotechnology and Bioengineering 33, 428–439.

Touvinen, O.H., Kelly, D.P., 1973. Studies on the growth of *Thiobacillus ferrooxidans*: I. Use of membrane filters and ferrous iron agar to determine viable number and comparison with CO_2 fixation and iron oxidation measures of growth. Archives on Microbiology 68, 285.